Ribosome hijacking: a role for small protein B during trans-translation.

Sylvie Nonin-Lecomte, Noella Germain-Amiot, Reynald Gillet, Marc Hallier, Luc Ponchon, Frédéric Dardel, Brice Felden

▶ **To cite this version:**

Sylvie Nonin-Lecomte, Noella Germain-Amiot, Reynald Gillet, Marc Hallier, Luc Ponchon, et al.. Ribosome hijacking: a role for small protein B during trans-translation.. EMBO Reports, 2009, 10 (2), pp.160-5. 10.1038/embor.2008.243 . inserm-00706654

HAL Id: inserm-00706654

https://www.hal.inserm.fr/inserm-00706654

Submitted on 11 Jun 2012

HAL is a multi-disciplinary open access archive for the deposit and dissemination of scientific research documents, whether they are published or not. The documents may come from teaching and research institutions in France or abroad, or from public or private research centers.

L'archive ouverte pluridisciplinaire **HAL**, est destinée au dépôt et à la diffusion de documents scientifiques de niveau recherche, publiés ou non, émanant des établissements d'enseignement et de recherche français ou étrangers, des laboratoires publics ou privés.

EMBO reports

scientific report

Ribosome hijacking: a role for small protein B during *trans*-translation

Sylvie Nonin-Lecomte[1*++], *Noella Germain-Amiot*[2*], *Reynald Gillet*[2], *Marc Hallier*[2], *Luc Ponchon*[1], *Frédéric Dardel*[1] & *Brice Felden*[2++]

[1]Laboratoire de Cristallographie et RMN Biologiques, CNRS UMR 8015, Université Paris Descartes, Paris, France, and
[2]UPRES JE2311, Inserm U835, Biochimie Pharmaceutique, Université de Rennes I, Rennes, France

Tight recognition of codon–anticodon pairings by the ribosome ensures the accuracy and fidelity of protein synthesis. In eubacteria, translational surveillance and ribosome rescue are performed by the 'tmRNA–SmpB' system (transfer messenger RNA–small protein B). Remarkably, entry and accommodation of aminoacylated-tmRNA into stalled ribosomes occur without a codon–anticodon interaction but in the presence of SmpB. Here, we show that within a stalled ribosome, SmpB interacts with the three universally conserved bases G530, A1492 and A1493 that form the 30S subunit decoding centre, in which canonical codon–anticodon pairing occurs. The footprints at positions A1492 and A1493 of a small decoding centre, as well as on a set of conserved SmpB amino acids, were identified by nuclear magnetic resonance. Mutants at these residues display the same growth defects as for Δ*smpB* strains. The SmpB protein has functional and structural similarities with initiation factor 1, and is proposed to be a functional mimic of the pairing between a codon and an anticodon.

Keywords: ribosome; decoding; *trans*-translation; tmRNA; SmpB
EMBO reports (2009) **10**, 160–165. doi:10.1038/embor.2008.243

INTRODUCTION

Protein synthesis occurs within the ribosome according to the rules of the genetic code (supplementary Fig S1a online). The 30S subunit ensures selection of the correct aminoacylated-transfer RNAs (aminoacylated-tRNAs). The 50S subunit catalyses the formation of the peptide bond. The decoding centre (DC) of the genetic information is within the 30S subunit. Translational accuracy and fidelity are ensured by key conserved nucleotides (Noller, 2006; A1492, A1493 of helix h44 and G530 of helix h18 of the 16S ribosomal RNA), which recognize the minihelix formed by the pairing of the cognate tRNA anticodon and the messenger RNA (mRNA; Ogle & Ramakrishnan, 2005). This induces a domain closure of the 30S for cognate tRNA and leads to GTP hydrolysis by elongation factor Tu approximately 75 Å away, allowing the acceptor branch of the tRNA to be accommodated into the acceptor A-site of the 50S subunit and the chemistry of peptidyl transfer to proceed.

In eubacteria and some organelles, these universal rules are temporarily broken during *trans*-translation, a translational surveillance mechanism, when the tmRNA–SmpB system (transfer messenger RNA–small protein B) performs the rescue of ribosomes stalled on defective mRNAs. The Ala-tmRNA functions as both a tRNA and an mRNA. With the help of SmpB and elongation factor Tu, it binds to the stalled ribosomes. Translation switches from mRNA to a short tmRNA internal open reading frame that encodes a degradation tag, leading successively to a normal termination, the release of the tagged polypeptide, and the disassembly and recycling of ribosomal subunits (Moore & Sauer, 2007). SmpB is an OB-fold protein; its carboxy terminal tail is essential for function (Jacob *et al*, 2005), but its structure is disordered outside the ribosome. Phylogenetically conserved residues define two surface patches on opposite sides of SmpB (Dong *et al*, 2002): one coincides with the surface that binds to the elbow region of the tRNA-like domain (TLD; Gutmann *et al*, 2003) and the other probably forms a contact with the ribosome.

Strikingly, the entry and accommodation of Ala-tmRNA into the A-site of a stalled ribosome occur in the absence of any codon–anticodon interaction. Indeed, tmRNA lacks an anticodon loop and can only enter the ribosome when the A-site is vacant. How can it bypass the decoding process and be accommodated for *trans*-peptidation is unknown. Solution probing (Kurita *et al*, 2007), cryo-electron microscopy (Gillet *et al*, 2007) and X-ray structures (Gutmann *et al*, 2003; Bessho *et al*, 2007) suggest that when *trans*-translation is initiated, one SmpB substitutes for a tRNA anticodon stem–loop within the A-site (supplementary

[1]Laboratoire de Cristallographie et RMN Biologiques, CNRS UMR 8015, Université Paris Descartes, 4, Avenue de l'Observatoire, 75006 Paris, France
[2]UPRES JE2311, Inserm U835, Biochimie Pharmaceutique, Université de Rennes I, 2 Avenue du Prof. L. Bernard, 35043, Rennes, France
*The authors contributed equally to this work
+Corresponding author. Tel: +33 1 53 73 15 74; Fax: +33 1 53 73 99 25; E-mail: sylvie.nonin@parisdescartes.fr
++Corresponding author. Tel: +33 2 23 23 48 51; Fax: +33 2 23 23 44 56; E-mail: brice.felden@univ-rennes1.fr

Received 4 June 2008; revised 30 October 2008; accepted 26 November 2008; published online 9 January 2009

 ©2009 EUROPEAN MOLECULAR BIOLOGY ORGANIZATION

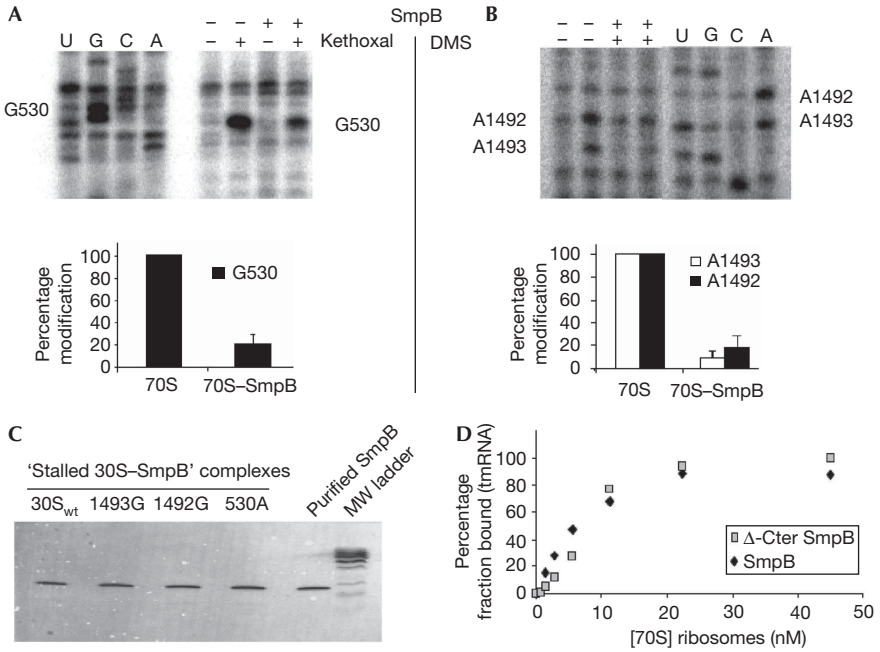

Fig 1 | Mapping of accessible Gs and As of *Escherichia coli* 16S ribosomal RNA within a stalled ribosome. (**A**) Kethoxal and (**B**) DMS. (Top) Autoradiograms of 12% polyacrylamide gels of the cleavage products of extended cDNAs. Lanes U, G, C and A: sequencing ladders. (Bottom) Quantification of the protections. (**C**) Immunoblotting of stalling 'truncated mRNA–tRNA^{fMet}–30S–SmpB' complexes from wt 30S or mutants at positions 530, 1492 and 1493. (**D**) Equilibrium dissociation experiments of tmRNA on stalled ribosomes from filter-binding assays, with maximum binding set to 1 and the other values expressed as the bound fraction: stalled 70S pre-loaded with wt SmpB (diamonds) or with Δ-Cter SmpB (squares). DMS, dimethylsulphate; mRNA, messenger RNA; SmpB, small protein B; tRNA, transfer RNA; tmRNA, transfer messenger RNA; wt, wild type.

Fig S1b online). *In vivo*, SmpB is associated with the stalled ribosomes independently of the presence of tmRNA, and pre-binding of SmpB to stalled ribosomes triggers *trans*-translation (Hallier *et al*, 2006).

Here, we show by chemical probing that the protein modifies the conformation of the universally conserved nucleotides A1492, A1493 and G530 of a stalled ribosome, and that the essential C-terminal tail of the protein interacts with G530, but that it is dispensable for the recruitment of tmRNA. We show that 30S mutants at these individual positions still bind to SmpB, indicating that the molecular recognition of the protein involves additional residues from the ribosome. By using nuclear magnetic resonance (NMR), within a ternary [TLD/SmpB/decoding centre] complex, we identify the interacting decoding centre nucleotides and SmpB residues. We show that strains expressing mutant SmpBs modified at the interacting positions display the same growth defects as those inactivated in *trans*-translation. On the basis of these data, a model of the interaction between the SmpB–TLD complex and the ribosomal A-site of the 30S subunit is inferred.

RESULTS

SmpB induces reactivity changes of the decoding site

We focused on the 16S ribosomal RNA (rRNA) loop 530 (h18) and on the top of h44 within stalled ribosomes, where SmpB fits roughly into the cryo-electron microscopy maps (Gillet *et al*, 2007). In the absence of SmpB, N1 and N2 of G530 are accessible to methylation by kethoxal. In the presence of wild-type SmpB, the reactivity decreases by about 80% (Fig 1A). The binding of a mutant deleted from the last 16 amino acids (**Δ**-Cter ecSmpB) leaves G530 accessible to modifications, showing that the C-terminal tail of SmpB either protects G530 or induces conformational changes at this position (data not shown). Similarly, A1492 N1 and A1493 N1 within the stalled ribosome are accessible to dimethylsulphate (DMS) modifications (Fig 1B), and their accessibility is reduced by about 80% on binding of wild-type ecSmpB. We conclude that SmpB reacts as a tRNA anticodon mimic during decoding by inducing reactivity changes at positions A1492, A1493 and G530.

Binding of SmpB to mutated 16S rRNA

Reactivity changes at G530, A1492 and A1493 on SmpB binding to a stalled ribosome led us to test SmpB binding to the 30S subunit carrying single-point mutations at each of these bases. The A1492G, A1493G and G530A mutations all result in dominant lethality and general translation defects in *Escherichia coli*. Each 30S mutant binds to SmpB in a manner similar to the wild-type 30S (Fig 1C), suggesting that the individual contributions of the three nucleotides to the molecular recognition of the 30S subunit by SmpB are negligible. Filter binding assays with labelled tmRNA, in complex with a stalled ribosomal complex preloaded with either wild-type or Δ-Cter ecSmpB, were performed to check whether the C terminus of SmpB influences the recruitment of tmRNA. The efficiency of both proteins is comparable

©2009 EUROPEAN MOLECULAR BIOLOGY ORGANIZATION

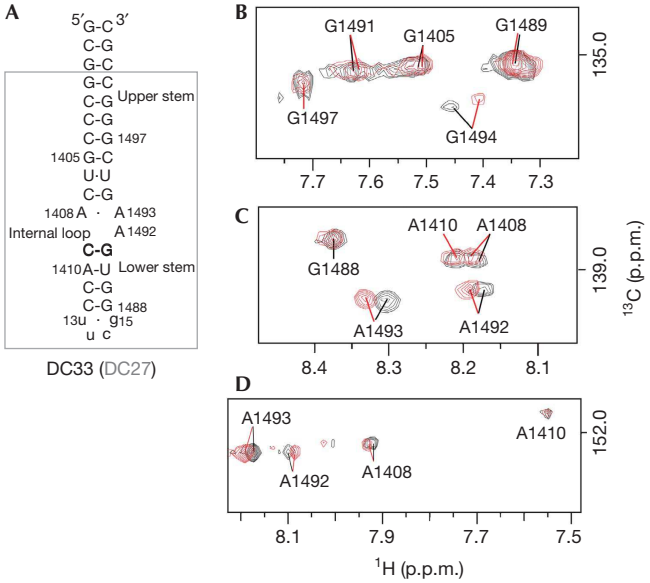

Fig 2 | Titration of ^{13}C,^{15}N-DC33 with (1:1) [TLD60/Δ-Cter SmpB]. (**A**) Two-dimensional structures of DC27 (boxed) and DC33. The three (DC27) or six (DC33) upper G-C base pairs, as well as the nucleotides 'uucg' from the apical loop, increase the stability of the RNA stem–loop and are not present in the natural sequences. (**B**–**D**) Overlays of selected regions of the ^{13}C–^{1}H HSQC spectra of the free RNA (black) and of ^{13}C, ^{15}N-DC33 in the presence of 8 equivalents of the (1:1) [TLD60/Δ-Cter SmpB] complex (red): (**B**,**C**) GH8 and AH8 regions; (**D**) AH2 region. DC, decoding center; HSQC, heteronuclear single quantum coherence spectroscopy; SmpB, small protein B.

(Fig 1D), showing that the 16 C-terminal residues are not essential during this early step, but seem to be required for pseudo-decoding.

SmpB interacts with TLD and the decoding centre

Ala-tmRNA accommodation proceeds in the absence of specific recognition by a complementary anticodon. On the basis of structural data, the RNA-binding site of the protein for the ribosomal decoding centre is predicted to be different from that of the TLD. We used the (1:1) [Δ-Cter SmpB/TLD60] complex to probe the SmpB–decoding centre interaction, focusing on a minimal decoding site encompassing A1492 and A1493, but excluding G530. The choices of the RNA sequences (DC27 and DC33; Fig 2) and of the protein (the *Aquifex aeolicus* Δ-Cter SmpB) are explained in the supplementary information online. Changes in the structure or dynamics of Δ-Cter SmpB and of DC33 on complex formation were probed using NMR under stringent ionic conditions (450 mM NaCl). The association of ^{15}N-labelled SmpB with TLD60 was monitored in an ^{1}H–^{15}N HSQC spectrum (HSQC for heteronuclear single quantum coherence spectroscopy; supplementary Fig S2a online). The NMR data are consistent with previous studies on the [SmpB/TLD] complex (Nameki *et al*, 2005; Bessho *et al*, 2007). Interacting residues are conserved among bacteria and are clustered on the 'top face' of the protein (supplementary Fig S3 online) within a region we called 'binding region 1' (BR1; supplementary information online).

We monitored the changes in the ^{1}H–^{15}N HSQC spectrum of SmpB on the addition of up to 8 equivalents of unlabelled DC27 RNA, using the (1:1) [Δ-Cter SmpB/TLD60] complex as a reference (Fig 3A). The induced chemical shift perturbation (CSP; Fig 3B and supplementary Fig S4a online) shows a second binding region (BR2) within the 'bottom face' of the protein, opposite to BR1, clustering along a stretch extending from L110 to K129, including residues Y20, L110, L112, K127 and K129 that are evolutionarily conserved.

The CSP in BR2 (supplementary Fig S4a online) originates from direct and indirect effects. Most residues of helix α1 (E15, A16, K19 and Y20) are strongly affected. Additional CSPs are located on β-sheets 6 (L110 and L112) and 7 (K118 and A124), both of which surround helix α1. In the free protein, the side chains of L110 and A124 point towards A16, forming hydrophobic interactions that could sense conformational changes in helix α1 on binding of the decoding centre. E102 from helix α3 is approximately 17 Å away from K19, which is compatible with the distance spacing of the A1492 and C1402 C1 atoms. K127, K129 and R134 are located in the flexible C-terminal part of the protein that protrudes from β-sheet 7, next to helix α1. Any conformational change within β-sheet 7 is expected to affect the conformation of the C-terminal tail of SmpB. In addition, these three basic residues could interact with the decoding centre.

The [SmpB–TLD] complex modifies the decoding site

Up to 8 equivalents of the (1:1) [Δ-Cter SmpB/TLD60] complex were added to ^{13}C,^{15}N-DC33 RNA in D_2O buffer. The corresponding ^{13}C–^{1}H HSQC spectra were compared with that of the free DC33 (Fig 2). The conformational changes induced by the protein extend to G1494 with its H8 resonance undergoing the largest CSP (Fig 2B). The aromatic resonances of neighbouring G1491 and A1408, which are part of the decoding centre, also shift to a lesser extent. The insignificant CSP observed for G1405 H8, G1497 H8, A1410 H8/H2, G1489 H8, G1488 H8 and g15 (data not shown) shows the preferential binding of SmpB to the decoding site, but not to the abutting stems. A1493 H8 CSP is larger than that of A1492 H8 (Fig 2C), which is in agreement with the probing data collected on a 70S ribosome (this study).

Mutations in the BR2 impair *trans*-translation

It is inferred from the NMR data that E15, K19, Y20, K127 and K129 of the *A. aeolicus* SmpB have a function in the interaction with the decoding centre. The biological relevance was assessed *in vivo* using the *E. coli* Δ*smpB* strains complemented with the ecSmpB mutants. Residues R19, E23, Y24, K131 and K133 are the homologues of the *A. aeolicus* residues E15, K19, Y20, K127 and K129, respectively. We constructed R19A/E23A/Y24A (ecSmpB-REY) and K131A/K133A (ecSmpB-KK) mutants. Complementation of a Δ*smpB* strain with wild-type *ecsmpB*, *ecsmpB-REY* or *ecsmpB-KK* genes yields similar levels of protein expression (data not shown). For the wild-type ecSmpB, the two ecSmpB variants associate with the 70S (the P100 fraction) and with tmRNA *in vivo* (supplementary Fig S5a online). However, they fail to complement the growth defect of the Δ*smpB* strain at 45 °C (supplementary Fig S5b online). The ecSmpB protein mutated at five residues from BR2, predicted from our NMR data to interact with the decoding centre, binds to the 70S and tmRNA, but presents a *trans*-translation-deficient phenotype *in vivo*.

©2009 EUROPEAN MOLECULAR BIOLOGY ORGANIZATION

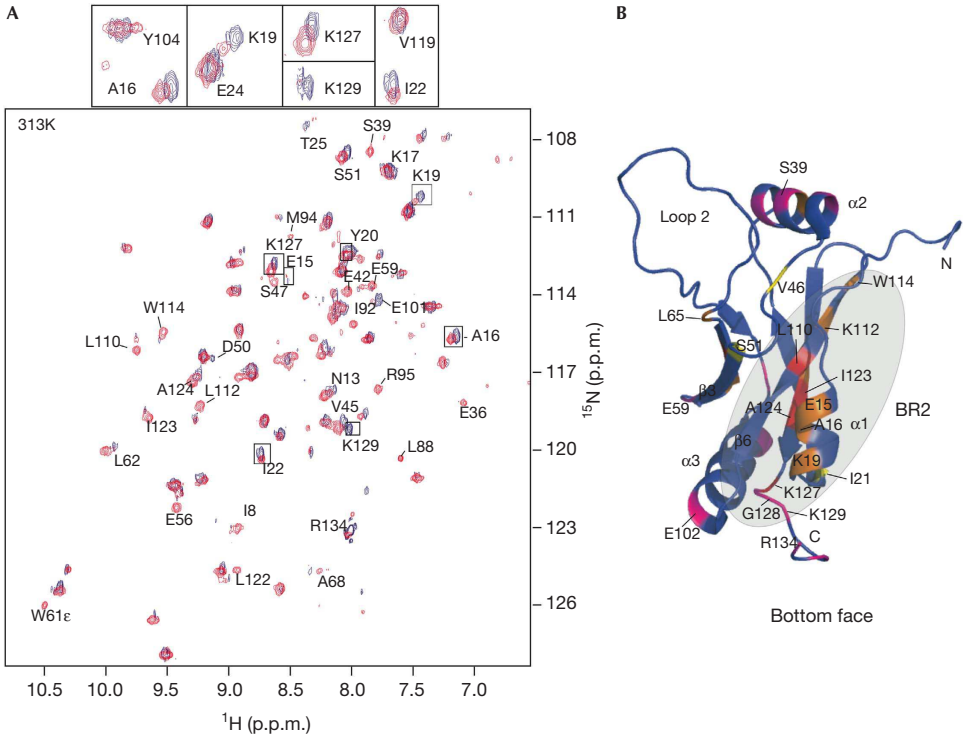

Fig 3 | DC27 binds to Δ-Cter SmpB region BR2. (**A**) Overlay of the ^{1}H–^{15}N HSQC spectra of Δ-Cter SmpB in the (1:1) [TLD60/Δ-Cter SmpB] complex (blue) and in the (1:1:8) [TLD60/Δ-Cter SmpB/DC27] complex (red). (**B**) Mapping of the perturbations onto the structure of SmpB (Protein Data Bank 1K8H1) using the colour code described in the Methods. BR2 is circled in grey. BR2, binding region 2; Cter, carboxyl terminus; DC, decoding centre; HSQC, heteronuclear single quantum coherence spectroscopy; SmpB, small binding protein B; TLD, transfer RNA-like domain.

Model of the 'SmpB–TLD–70S ribosome' complex

We combined the published crystallographic data with our study to propose a model of the 'SmpB–TLD' complex into a 70S ribosome, consistent with the one reported by Bessho *et al* (2007) and with the cryo-electron microscopy data (Kaur *et al*, 2006), and with all our NMR and probing results. The docking procedure is described in the supplementary information online. In the resulting model (Fig 4), SmpB fills the space normally occupied by the anticodon stem–loop of the A-site tRNA. The localization of helix α1 and of some conserved residues at the end of β-sheet 7 suggests that these parts of SmpB can contact with A1492, A1493 and G530.

DISCUSSION

SmpB mimics a codon–anticodon pairing

Recent cryo-electron microscopy reconstructions (Gillet *et al*, 2007) and hydroxyl radical probing of the interaction between SmpB and ribosomes (Kurita *et al*, 2007) suggest that SmpB binds to the 30S near the decoding centre (supplementary Fig S1 online). Our structural and biochemical data suggest that the tmRNA–SmpB complex acts as a 'codon–anticodon' mimic during *trans*-peptidation of the stalled polypeptide to the tmRNA alanine. Conserved G530, A1492 and A1493 contact a cognate 'codon–anticodon' pair by induced fit during decoding. Here, we have shown that SmpB protects the Watson–Crick positions of these three bases within a stalled ribosomal complex, as does a tRNA anticodon stem–loop. Each of these bases can be mutated without impairing the binding of SmpB to the ribosome, implying that their contributions to binding are limited. Although having no contribution to the recruitment of tmRNA to the ribosome, the C terminus of SmpB is essential for *trans*-peptidation (Hallier *et al*, 2006). The absence of *trans*-translation when the SmpB C-terminal tail is lacking is due to defects occurring after the recruitment of tmRNA, but before or during *trans*-peptidation. The NMR data using a ΔC-ter SmpB support a suggested orientation of the protein in which its globular body interacts with the top of h44 containing A1493, whereas its C-terminal tail points towards h18, along with the mRNA path (Kurita *et al*, 2007). Our data suggest that the C-terminal tail of SmpB has an important contribution during pseudo-decoding, owing to interactions with G530. Close interactions of the C-terminal extension in the vicinity of G530 might help to trigger pseudo-decoding.

Similarities between SmpB and Initiation factor 1

Our data are consistent with the functional conformational changes of the three conserved bases from the decoding centre on SmpB binding to the stalling complex. Remarkably, our NMR and probing data show that the conformation of A1492 and A1493 is modified in the presence of a 'TLD–SmpB' complex. Until now, these changes were detected on the pairing of an mRNA codon to a tRNA anticodon (Ogle *et al*, 2001), on binding of Initiation factor 1 (IF1; Carter *et al*, 2001) or of aminoglycosides (Fourmy *et al*, 1998; Ogle *et al*, 2001). Both SmpB and IF1 are members of the S1 family of OB-fold proteins (Dong *et al*, 2002).

©2009 EUROPEAN MOLECULAR BIOLOGY ORGANIZATION

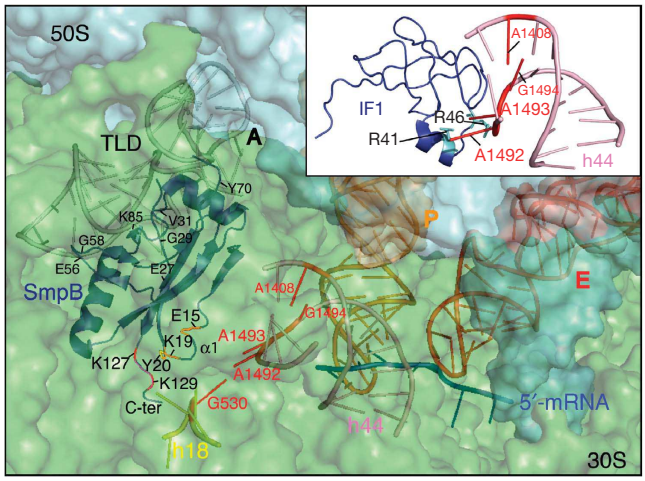

Fig 4 | Model of the decoding centre–SmpB interaction within the ribosome. 50S and 30S subunit surfaces from a *Thermus thermophilus* ribosome are shown in cyan and pale green, respectively; E-site and P-site tRNAs in red and orange; mRNA in blue; TLD in grey; and SmpB in blue. The parts of h44 and h18 involved in the decoding are shown in ribbon mode (pink and yellow). Adenines 1408, 1492, 1493 from h44 and G530 from h18 are in red. BR2 SmpB amino acids are coloured as in Fig 2. (Inset) Comparison with the IF1 structure (purple) with the decoding site (pink, PDB 1HR0). Red: decoding centre A1408, A1492 and A1493; cyan: R41 and R46 stack against the A1492 and A1493, respectively. BR2, binding region 2; IF1, Initiation factor 1; SmpB, small protein B.

IF1 interacts with the 30S, especially within the decoding centre, through a loop inserting into the h44 minor groove and flipping out bases A1492 and A1493, and tight interactions with the phosphate backbone of the h18 G530 loop. A1492G and A1493G ribosomal mutations disrupt IF1 binding to the 30S, whereas G530A allows IF1 binding. Conversely, and as shown here, the SmpB binding is retained, suggesting that the protein has other anchor points, including its C-terminal domain. The IF1 structure in complex with the decoding centre (PDB 1HRO) was docked into our stalling model by superimposing the decoding centre internal loops from the 16S rRNA (Fig 4, inset). Strikingly, an alpha helix rich in basic residues is found in the vicinity of both the IF1- and SmpB-interacting domains with the decoding centre, even though the orientations of the two helices are different. Furthermore, the positioning of R41 and R46 in IF1, and the distance between them are consistent with the identified residues of BR2. Our model suggests that residues E15, K19 and Y20 induce and/or stabilize A1492 and A1493 conformational changes, as for IF1 R41 and R46. The functional relevance of our structural results was supported by an *E. coli* strain expressing the A19-A23-Y24 triple ecSmpB mutant that has a growth defect similar to that of a ΔSmpB strain (supplementary Fig S5b online), supporting the essential role of some (or all) of these residues for the function of SmpB. In the ternary complex, significant CSP was also observed for K127, K129 and R134 (Fig 2), expected to interact with the decoding centre (Fig 4). Our model orientates K127 and K129 towards G530, and towards the mRNA path (Fig 4) suggesting that they might act as a guide for the correct positioning of SmpB within an empty A-site.

It is likely that SmpB reorientates slightly during accommodation. We hypothesize that this would drive conformational changes within the TLD that could be the trigger for GTP hydrolysis and subsequent peptidyl transfer. The fate of SmpB after translocation of tmRNA to the P-site is of particular interest. A second binding site for SmpB is present within the 30S P site (Ivanova *et al*, 2005; Kurita *et al*, 2007). After peptidyl transfer, the translocation of tmRNA to the P-site might occur in complex with SmpB, still mimicking a 'codon–anticodon' interaction. Such a model would allow the exit of the protein from the ribosome by the E-site, after an additional round of translation.

METHODS

Preparation and purification of the complexes. Complexes of *E. coli* ribosomes with P-site tRNA stalled on the rGGCAAGG AGGUAAAAAUG mRNA sequence and mutant 30S subunits were prepared as described previously (Valle *et al*, 2003; Hallier *et al*, 2006), using a fourfold or twofold excess of either wild-type or Δ-Cter (Hallier *et al*, 2006) SmpBs, respectively. The protein was incubated for 15 min at 37 °C and purified on a Superdex 200 HR 10/30 column (GE Healthcare, Orsay, France). Anti-SmpB Western blots were performed as described by Hallier *et al* (2006).

Chemical modifications. DMS and kethoxal methylations were achieved as described by Stern *et al* (1988). Primer extensions were performed using 5′-ACGGTTACCTTGTTA-3′ and 5′-CGTGCGCTTTACGCCCA-3′, complementary to nucleotides 1512–1498 and 565–581 of 16S rRNA, respectively. Annealing to the purified rRNA was in Tris–HCl 50 mM pH 8.3, NaCl 60 mM and dithiothreitol 10 mM by heating at 96 °C for 40 s followed by ice freezing for 1 min. Extension was performed by adding 0.5 U of the AMV reverse transcription in Tris–HCl 50 mM pH 8.3, NaCl 60 mM, $MgCl_2$ 6 mM and dithiothreitol 10 mM. After 30 min at 45 °C, samples were analysed by polyacrylamide gel electrophoresis together with the sequencing of the *E. coli* 16S rRNA.

Equilibrium dissociation experiments. After folding, 2 μl [γ^{32}P]tmRNA was added to the ribosomal complexes and left for 5 min at 20 °C, in 15 μl of 5 mM Hepes-KOH, pH 7.5, 50 mM KCl, 10 mM NH_4Cl, 10 mM MgOAc and 6 mM β-mercaptoethanol. The samples were diluted with 500 μl of ice-cooled buffer, filtered over nitrocellulose filters and washed with 3 × 1 ml of the same buffer. Membranes were dried and radioactivity was measured.

NMR. DC27 RNA was purchased from Perbio (Brebieres, France). ^{13}C–^{15}N DC33, TLD60 and the *A. aeolicus* Δ-Cter SmpB were overproduced and purified as described by Gaudin *et al* (2003), Gutmann *et al* (2003) and Ponchon & Dardel (2007). The NMR buffer for the pure RNA and protein samples is 95%H_2O–5% H_2O, 450 mM NaCl, 0.1 mM EDTA, pH 6.5. When necessary, H_2O was exchanged for D_2O. The concentration of the reference molecule was set to 0.2 mM. All RNA sample tubes were heated and snap-cooled before NMR experiments. Spectra were recorded on a 600 MHz Bruker advance spectrometer equipped with a TXI probe, using 5 mm Shigemi NMR tubes, processed with NMRPipe (Delaglio *et al*, 1995) and analysed with Sparky. Specific amide NH assignments were checked and reassigned on the basis of the assignments at lower salt concentrations and standard ^{1}H–^{15}N HSQC, ^{15}N NOESY (nuclear Overhauser effect spectroscopy)-HSQC and ^{15}N TOCSY (total correlation spectroscopy)-HSQC

©2009 EUROPEAN MOLECULAR BIOLOGY ORGANIZATION

experiments. The NMR titration protocol is provided in the supplementary information online. The changes in the chemical shifts of the amide ^{1}H and ^{15}N were averaged by using the formula: $wacs = \{[1/2[(\Delta H)^2 + (0.2\Delta N)^2]]\}^{1/2}$ (Foster *et al*, 1998) and plotted against the residue number. The cutoff value (c.o.) of $+\sigma$ was computed. All residues undergoing wacs > c.o. were mapped in red on the structure, and those with wacs in the ranges [c.o.−90% c.o] and [90% c.o.−80% c.o.] in orange and yellow, respectively. Amino acids with NH cross-peak broadened to baseline were mapped in magenta. The structures of the ribosome, as well as of SmpB and of IF1 proteins, were displayed using PYMOL (Delano, 2002) and subjected to manual docking as explained in the supplementary information online.

Supplementary information is available at *EMBO reports* online (http://www.emboreports.org)

ACKNOWLEDGEMENTS

We are grateful to Dr A. Méreau (Unité Mixte de Recherche (UMR)6061, Rennes) for help in the probing experiments, and Bili Seijo (UMR8015) for help in sample preparation. The 30S mutants were provided by Dr R. Green (Johns Hopkins University, USA). This study was supported by grants from Région Bretagne (PRIR Grant no. 691 and CRB 2004-1483), Action Concertée Incitative BCMS 136 and Agence Nationale de la Recherche programme MIME 2006 to B.F.

CONFLICT OF INTEREST

The authors declare that they have no conflict of interest.

REFERENCES

Bessho Y, Shibata R, Sekine S, Muruyama K, Higashijima K, Hori-takemoto C, Shirouzu M, Kuramitsu S, Yokoyama S (2007) Structural basis for functional mimicry of long-variable-arm tRNA by transfer-messenger RNA. *Proc Natl Acad Sci USA* **104:** 8293–8298

Carter A, Clemons WM Jr, Brodersen DE, Morgan-Warren RJ, Hartsch T, Wimberly BT, Ramakrishnan V (2001) Crystal structure of an initiation factor bound to the 30S ribosomal subunit. *Science* **291:** 498–501

Delaglio F, Grzesiek S, Vuister GW, Zhu G, Pfeifer J, Bax A (1995) NMRPipe: a multidimensional spectral processing system based on UNIX pipes. *J Biomol NMR* **6:** 277–293

DeLano WL (2002) *The PyMOL Molecular Graphics System*. San Carlos, CA, USA: DeLano Scientific LLC http://www.pymol.org

Dong G, Nowakowski J, Hoffman DW (2002) Structure of small protein B: the protein component of the tmRNA–SmpB system for ribosome rescue. *EMBO J* **21:** 1845–1854

Foster MP, Wuttke DS, Clemens KR, Jahnke W, Radhakrishnan I, Tennant L, Reymond M, Chung J, Wright PE (1998) Chemical shift as a probe of molecular interfaces: NMR studies of DNA binding by the three amino-terminal zinc-finger domains from transcription factor IIIA. *J Biomol NMR* **12:** 51–71

Fourmy D, Recht MI, Puglisi JD (1998) Binding of neomycin-class aminoglycoside antibiotics to the A-site of 16 S rRNA. *J Mol Biol* **277:** 347–362

Gaudin C, Nonin-Lecomte S, Tisné C, Corvaisier S, Bordeau V, Dardel F, Felden B (2003) The tRNA-like domains of *E. coli* and *A. aeolicus* transfer-messenger RNA: structural and functional studies. *J Mol Biol* **331:** 457–471

Gillet R, Kaur S, Li W, Hallier M, Felden B, Frank J (2007) Scaffolding as an organizing principle in *trans*-translation. *J Biol Chem* **282:** 6356–6363

Gutmann S, Haebel PW, Metzinger L, Sutter M, Felden B, Ban N (2003) Crystal structure of the transfer-RNA domain of transfer-messenger RNA in complex with SmpB. *Nature* **424:** 699–703

Hallier M, Desreac J, Felden B (2006) Small protein B interacts with the large and the small subunits of a stalled ribosome during *trans*-translation. *Nucleic Acids Res* **34:** 1935–1943

Ivanova N, Pavlov MY, Bouakaz E, Ehrenberg M, Schiavone LH (2005) Mapping the interaction of SmpB with ribosomes by footprinting of ribosomal RNA. *Nucleic Acids Res* **33:** 3529–3539

Jacob Y, Sharkady SM, Bhardwaj K, Sanda A, Williams KP (2005) Function of the SmpB tail in transfer-messenger RNA translation revealed by a nucleus-encoded form. *J Biol Chem* **280:** 5503–5509

Kaur S, Gillet R, Li W, Gursky R, Frank J (2006) Cryo-EM visualization of transfer messenger RNA with two SmpBs in a stalled ribosome. *Proc Natl Acad Sci USA* **103:** 16484–16489

Kurita D, Sasaki R, Muto A, Himeno H (2007) Interaction of SmpB with ribosome from directed hydroxyl radical probing. *Nucleic Acids Res* **35:** 7248–7255

Moore SD, Sauer RT (2007) The tmRNA system for translational surveillance and ribosome rescue. *Annu Rev Biochem* **76:** 101–124

Nameki N *et al* (2005) Interaction analysis between tmRNA and SmpB from *Thermus thermophilus*. *J Biochem* **138:** 729–739

Noller HF (2006) Evolution of ribosomes and translation from an RNA world. In *The RNA World,* Gesteland RF, Cech TR, Atkins JF (eds) 3rd edn, Chapter 10, pp 287–307. Cold Spring Harbor, New York, USA: Cold Spring Harbor Laboratory Press

Ogle JM, Ramakrishnan V (2005) Structural insights into translational fidelity. *Annu Rev Biochem* **74:** 129–177

Ogle JM, Brodersen DE, Clemons WM Jr, Tarry MJ, Carter AP, Ramakrishnan V (2001) Recognition of cognate transfer RNA by the 30S ribosomal subunit. *Science* **292:** 897–902

Ponchon L, Dardel F (2007) Recombinant RNA technology: the tRNA scaffold. *Nat Methods* **4:** 571–576

Stern S, Moazed D, Noller HF (1988) Structural analysis of RNA using chemical and enzymatic probing monitored by primer extension. *Methods Enzymol* **164:** 481–489

Valle M, Gillet R, Kaur S, Henne A, Ramakrisnan V, Frank J (2003) Visualizing tmRNA entry into a stalled ribosome. *Science* **300:** 127–130

©2009 EUROPEAN MOLECULAR BIOLOGY ORGANIZATION